

RSC Advances



This is an *Accepted Manuscript*, which has been through the Royal Society of Chemistry peer review process and has been accepted for publication.

Accepted Manuscripts are published online shortly after acceptance, before technical editing, formatting and proof reading. Using this free service, authors can make their results available to the community, in citable form, before we publish the edited article. This *Accepted Manuscript* will be replaced by the edited, formatted and paginated article as soon as this is available.

You can find more information about *Accepted Manuscripts* in the [Information for Authors](#).

Please note that technical editing may introduce minor changes to the text and/or graphics, which may alter content. The journal's standard [Terms & Conditions](#) and the [Ethical guidelines](#) still apply. In no event shall the Royal Society of Chemistry be held responsible for any errors or omissions in this *Accepted Manuscript* or any consequences arising from the use of any information it contains.

Structures and bonding of auropolyboroenes $[\text{Au}_2(\text{B}_4)_x\text{B}_3]^-$, $[\text{Au}_2(\text{B}_4)_x\text{B}_2]^{2-}$ and $[\text{Au}_2(\text{B}_4)_x\text{B}]^+$ ($x = 2, 3$): Comparison with dihydride polyboroenes

Peng Shao^{a,*}, Li-Ping Ding^a, Cheng Lu^b, Jiang-Tao Cai^a, Bo Liu^a and Chang-Bo Sun^a

Abstract

Equilibrium structures of auropolyboroenes $[\text{Au}_2(\text{B}_4)_x\text{B}_3]^-$, $[\text{Au}_2(\text{B}_4)_x\text{B}_2]^{2-}$ and $[\text{Au}_2(\text{B}_4)_x\text{B}]^+$ ($x = 2, 3$) are obtained from density functional theory-based calculation. Results show that the ground states of Au_2B_9^+ , $\text{Au}_2\text{B}_{13}^+$ and $\text{Au}_2\text{B}_{14}^{2-}$ can be obtained by adding two Au atoms on the corresponding ground-state pure boron clusters. For $\text{Au}_2\text{B}_{10}^{2-}$, $\text{Au}_2\text{B}_{11}^-$, $\text{Au}_2\text{B}_{14}^{2-}$ and $\text{Au}_2\text{B}_{15}^-$, the ladder structures are proved to be the ground states at TPSS, OVGf, and CCSD(T) levels, which is similar to that of dihydride polyboroenes. AdNDP analysis indicates that the two rows of boron atoms in these auropolyboroenes are bonded by delocalized three-, four-, or five-center σ and π bonds. Especially, the dominant bonding patterns in $\text{Au}_2\text{B}_{11}^-$ and $\text{Au}_2\text{B}_{14}^{2-}$ bear similarities to those of dihydride polyboroenes. The photoelectron spectroscopy (PES) spectra for anionic clusters were simulated to facilitate the experimental PES spectra. In addition, the fragmentation energies and products against different decay channels are estimated and discussed.

1. Introduction

Over the past decades, pure boron clusters have attracted considerable attention because the boron possesses interesting chemical bonding properties and plays essential roles in advancing chemical bonding models.^{1,2} A series of joint experimental and theoretical studies have presented that all the boron clusters possess planar or quasi-planar geometries in their ground states up to very large sizes.³⁻¹⁶ For the cations, the transitions from planar or quasi-planar to three-dimensional (3D) structure occur at B_{16}^+ ,¹⁵ at B_{20} for the neutrals¹² and at least up to B_{23}^- for the

^a College of Science, Shaanxi University of Science & Technology, Xi'an 710021, China

^b Department of Physics, Nanyang Normal University, Nanyang 473061, China

*Correspondence to: Peng Shao, College of Science, Shaanxi University of Science & Technology, Xi'an 710021, China.

E-mail address: scu_sp@163.com (Peng Shao).

anions⁸⁻¹³, where the exact size for the anions is still unclear. Furthermore, boron clusters have been tested to possess the rich chemical bonding properties, which can be understood based on the π and σ aromaticity and antiaromaticity. Boron-based material, especially boron hydrides (boranes), have been popular due to they can store a good amount of hydrogen and release it upon chemical treatment when needed¹⁷. To explain the structure of all known boron hydrides, Longuet-Higgins, Lipscomb and co-workers^{18,19} first put forward the concept of three-center two-electron (3c-2e) bonding. The 3c-2e bond represents a milestone in establishing the validity of the molecular orbital theory. From then on, a surge of studies were devoted to the structure and chemical bonding of boranes. Additionally, the electron delocalization and aromaticity have also been proved to be key bonding features for the electron-deficient boranes.

In previous studies, Au/H similarity is well supported by surprising experimental discovery of H/AuPR₃ analogy²⁰. Further analogy between a bare Au atom and H has also been discovered in gas-phase binary Au clusters.²¹⁻²³ The analogy extended the structures and bonding in variety of boron-hydrides to B-Au compounds. Such as the heptaboron aurides B₇Au₂⁻ anion²² was first studied by Zhai *et al.* using photoelectron spectroscopy and ab initio calculations in 2006. The results showed that B₇Au₂⁻ possesses an extremely stable planar structure, which is identical to that of B₇H₂⁻. What's more, the B-Au bonding was shown to be covalent, similar to the B-H bonding, indicating the Au mimics H in its bonding to boron. A subsequent study²³ via density functional theory calculations showed that the closo-auroboranes B_xAu_x²⁻ ($x = 7-14$) dianions possess structure and bonding analogous to the famous deltahedral closo-borane cages, B_xH_x²⁻, demonstrating the Au indeed similar to H. In 2010, Zhai groups²⁴ found that the highly covalent B-Au bond in B₁₀Au⁻ is also similar to the B-H bond in B₁₀H⁻. The BAu_n^{0/-} ($n = 1-4$)²⁵ and B₂Au_n^{0/-} ($n = 1, 3, 5$)²⁶ auroboranes have also been proved to possess similar geometrical structures and bonding patterns with corresponding boron hydrides. More recently, Chen *et al.*²⁷ studied B₆Au_n^{0/-} ($n = 1-3$), which provide new examples for the Au/H analogy in Au alloy clusters. These studies on B-Au clusters all indicate that Au serve as monovalent σ ligand apes

hydrogen.

The investigations mentioned above unquestionably provide precious information on Au/H analogy, as well as the structure and chemical bonding of boron-gold alloy clusters. However, the previous studies only limited to neutral and anionic B-Au compounds. In the current study, we report a new specie cations with the stable closed structures, such as $[\text{Au}_2(\text{B}_4)_x\text{B}]^+$ in combination with $[\text{Au}_2(\text{B}_4)_x\text{B}_3]^-$ and $[\text{Au}_2(\text{B}_4)_x\text{B}_2]^{2-}$ ($x = 2, 3$) auropolyboroenes. In previous investigation, Li et al.²⁸ have conjectured that $[\text{H}_2(\text{B}_4)_x\text{B}_3]^-$, $[\text{H}_2(\text{B}_4)_x\text{B}_2]^{2-}$ and $[\text{H}_2(\text{B}_4)_x\text{B}]^+$ should possess similar characteristics with the stable closed-shell H_2B_7^- , $\text{H}_2\text{B}_{10}^{2-}$, H_2B_9^+ species, respectively. Taking Au/H analogy into account, we think the corresponding auropolyboroenes should also show interesting properties. In this case, we performed quantum chemical calculations on the auropolyboroenes $[\text{Au}_2(\text{B}_4)_x\text{B}_3]^-$, $[\text{Au}_2(\text{B}_4)_x\text{B}_2]^{2-}$, $[\text{Au}_2(\text{B}_4)_x\text{B}]^+$ ($x = 2, 3$) using density functional theory (DFT) method to address several issues. (1) What patterns of structure and chemical bonding exist in them? (2) Whether they are high stable molecules? (3) Whether their bonding pattern bear similarities to those in dihydride polyboroenes especially for cations. Additionally, in order to facilitate the synthesis of auropolyboroenes in the bulk or deposited on surfaces, we have calculated vertical detachment energy (VDE) for the concerned anions and adiabatic ionization potentials (AIP) for neutrals. Meanwhile, the most preferred fragmentation channels and products were also predicted.

2. Computational methods

Using density functional theory (DFT) method TPSS with the τ -dependent gradient-corrected functional²⁹, as implemented in *GAUSSIAN09* codes,³⁰ we performed quantum chemical calculations for auropolyboroenes $[\text{Au}_2(\text{B}_4)_x\text{B}_3]^-$, $[\text{Au}_2(\text{B}_4)_x\text{B}_2]^{2-}$ and $[\text{Au}_2(\text{B}_4)_x\text{B}]^+$ ($x = 2, 3$). The Stuttgart/Bonn relativistic effective core (SDD)³¹ was adopted for gold atom, and all-electron 6-311+G* basis set³² with polarization and diffuse functions for boron and hydrogen atoms. The reliability and accuracy of functional form was first guided by extensive tests performed on two-atom clusters (Au_2 , B_2 , AuB and AuB^-), using a variety of methods (the hybrid DFT methods: B3LYP³³, B3PW91³³⁻³⁵; the DFT methods: TPSS²⁹, PBE³⁶, BPW91³⁴,

³⁷, and PW91^{33, 34}; M06³⁸ and CCSD³⁹⁻⁴¹). The tested results combined with the corresponding experimental values and reliable theoretical values are summarized in Table 1. According to the results we found that the bond length and frequency of Au₂ and B₂ based on the TPSS/Au/SDD/B/6-311+G* level are in good agreement with the experimental values.⁴²⁻⁴⁴ The TPSS results for AuB and AuB⁻ dimers were also comparable with other DFT functions and ab initio calculations²⁵ which further validate our selected methods.

Our recipe for finding the equilibrium structures of auropolyboroenes is as follows. The geometries of pure B₉⁺, B₁₀²⁻, B₁₁⁻, B₁₃⁺, B₁₄²⁻ and B₁₅⁻ clusters were first optimized referring to various previous reported structures⁴⁵⁻⁴⁷. To search for the lowest energy structure of auropolyboroenes, a large number of initial structures were obtained by placing the gold atoms on each possible site of corresponding pure boron clusters as well as by substituting two B atoms using Au in B_{n+2}^{+/-} clusters. Then, the simulated photoelectron spectroscopy spectra for obtained anionic isomers were performed and compared with available experimental spectra²⁸. In the geometry optimization procedure, different possible spin multiplicities were also taken into account for each of these isomers. All the structure optimizations were carried out without any symmetry constraints. Finally, we performed the vibrational frequency computations to ensure that the optimized geometry corresponds to a local minimum in potential energy. Afterwards, the first two lowest-energy isomers obtained at TPSS theory method were recalculated by high-quality methods such as CCSD(T)⁴⁸ and the outer valence Green's function (OVGF)⁴⁹⁻⁵¹. The vertical detachment energy and adiabatic ionization potentials (VDE and AIP) were calculated by the TPSS function. The chemical bonding analysis was also performed using the adaptive natural density partitioning (AdNDP) method^{52, 53} as implemented in the Multiwfn 3.1 program⁵⁴. Molecular orbital visualization was done using the Gaussview 5.0.8 program⁵⁵.

3. Results and discussion

3.1. Geometrical structures

3.1.1. Pure multicharged B₉⁺, B₁₀²⁻, B₁₁⁻, B₁₃⁺, B₁₄²⁻ and B₁₅⁻ clusters

Based on the method mentioned above, we try our best to search for the

equilibrium structures of auropolyborenes $[\text{Au}_2(\text{B}_4)_x\text{B}_3]^-$, $[\text{Au}_2(\text{B}_4)_x\text{B}_2]^{2-}$ and $[\text{Au}_2(\text{B}_4)_x\text{B}]^+$ ($x = 2, 3$). The first step is to optimize the geometric structures of pure multicharged B_9^+ , B_{10}^{2-} , B_{11}^- , B_{13}^+ , B_{14}^{2-} and B_{15}^- clusters. These pure boron clusters have been well studied by many DFT investigations in previous literatures⁴⁵⁻⁴⁷ except for B_{14}^{2-} cluster. In this work, although all the possible isomers of bare boron clusters for each cluster size were extensively explored, only the first two lowest energy geometric structures were shown in Fig. 1. The first and second lowest energy isomers are designated by a lowercase letter a, b. It is worth pointing out that the ground state structures for each cluster are in good agreement with the results given by ref. 45-47. For B_{14}^{2-} dianion, there is no detailed geometry available. Our obtained ground state geometry of B_{14}^{2-} has ladderlike structure with high point symmetry C_{2h} , whereas for the other clusters, the ladderlike structures are less stable than the ground states in energy.

3.1.2. Auropolyborenes $[\text{Au}_2(\text{B}_4)_x\text{B}_3]^-$, $[\text{Au}_2(\text{B}_4)_x\text{B}_2]^{2-}$ and $[\text{Au}_2(\text{B}_4)_x\text{B}]^+$ ($x = 2, 3$)

In this section, we discuss the structural details of low-lying isomers of auropolyborenes Au_2B_9^+ , $\text{Au}_2\text{B}_{10}^{2-}$, $\text{Au}_2\text{B}_{11}^-$, $\text{Au}_2\text{B}_{13}^+$, $\text{Au}_2\text{B}_{14}^{2-}$ and $\text{Au}_2\text{B}_{15}^-$ which are obtained at TPSS/Au/SDD/B/6-311+G* level. During the geometry optimizations, a large number of optimized isomers for auropolyborenes are obtained by adding two gold atoms on each possible site of the corresponding pure boron clusters. We only selected the first two low-lying isomers for each type and listed them together with their point symmetries, electron states and some bond lengths in Fig. 2. Results of our final relative energies for the first and second local minima at three levels of theory TPSS, OVGF and CCSD(T) are also summarized in this figure. Some additional higher-energy isomers along with their information are given in Fig. S1, Fig. S2 and Fig. S3 of supplementary information. To distinguish the different structures, these isomers for each species are followed by a lowercase letter a, b, c, d, ... representing their energies from low to high. The calculated vertical detachment energies and adiabatic ionization potentials (VDEs and AIPs) for the ground state structures are gathered in Table 2. In addition, the ground states of the corresponding dihydride polyborenes H_2B_9^+ , $\text{H}_2\text{B}_{10}^{2-}$, $\text{H}_2\text{B}_{11}^-$, $\text{H}_2\text{B}_{13}^+$, $\text{H}_2\text{B}_{14}^{2-}$ and $\text{H}_2\text{B}_{15}^-$ are also

obtained at the same theory level and collected in Fig. S4 of supplementary information as comparison.

As is shown in Fig. 2, our most stable Au_2B_9^+ -a structure has C_s symmetry with two Au atoms bind associatively (dimer like) to different binding sites. It lies 0.13, 1.31 and 0.16 eV lower than the next lowest isomer (Au_2B_9^+ -b) at TPSS, OVGF and CCSD(T) levels, respectively. The calculated Au–Au bond length (2.72 Å) of Au_2B_9^+ -a is longer than the equilibrium Au–Au distance (2.47 Å) in isolated Au_2 , whereas it is shorter than the Au–Au distance (2.884 Å) in bulk Au. The second low-lying isomer Au_2B_9^+ -b has two Au atoms separately connected to the ladder structure of pure boron B_9^+ -b isomer. This structure is similar to the ground state of H_2B_9^+ (Fig. S4) obtained by us at TPSS/6-311+G* level. For the cationic $\text{Au}_2\text{B}_{13}^+$ auropolyboroene, the ground state can be obtained by adding two Au atoms on the apexes of the low-lying isomer of B_{13}^+ (Ref. 46). In other words, the B_{13}^+ moiety retains intact except for minor distortions. It is followed by a ladder structure ($\text{Au}_2\text{B}_{13}^+$ -e) with high C_{2v} point symmetry, which is 0.72 eV higher in energy at TPSS level. However, for the four negatively charged auropolyboroenes $\text{Au}_2\text{B}_{10}^{2-}$, $\text{Au}_2\text{B}_{11}^-$, $\text{Au}_2\text{B}_{14}^{2-}$ and $\text{Au}_2\text{B}_{15}^-$, the ladderlike structures were proved to be the ground states at three theory levels TPSS, OVGF, and CCSD(T). Among these ground state structures, there is a very interesting phenomenon. For even numbered boron clusters, the two Au atoms attached terminally to the corresponding pure B_{10}^{2-} and B_{14}^{2-} dianions in a trans fashion; while for odd numbered ones, the two Au atoms are in the cis position. In addition, the structures of these lowest-energy isomers are nearly identical to the ground state structures of $\text{H}_2\text{B}_{10}^{2-}$, $\text{H}_2\text{B}_{11}^-$, $\text{H}_2\text{B}_{14}^{2-}$ and $\text{H}_2\text{B}_{15}^-$ as shown in Fig. S4. This further provides new examples for Au/H analogy in Au alloy clusters. Thus, comparing with the stable closed-shell $\text{H}_2\text{B}_{10}^{2-}$, H_2B_9^+ species²⁸ and our obtained dihydride polyboroenes at TPSS level, we can conclude that these closed-shell auropolyboroenes considered in present work are all stable. It is worth mentioning that among these four auropolyboroenes, only the ground state of $\text{Au}_2\text{B}_{14}^{2-}$ can be obtained by adding two Au atoms to the lowest-energy structure of B_{14}^{2-} , while the ground states of $\text{Au}_2\text{B}_{10}^{2-}$, $\text{Au}_2\text{B}_{11}^-$ and $\text{Au}_2\text{B}_{15}^-$ is obtained by bonding two Au atoms

to the second lowest-energy isomer of pure boron clusters. Moreover, for $\text{Au}_2\text{B}_{10}^{2-}$, $\text{Au}_2\text{B}_{11}^-$, $\text{Au}_2\text{B}_{14}^{2-}$ and $\text{Au}_2\text{B}_{15}^-$ clusters, we found that the structures with two Au atoms binding associatively are higher in energy than that with two Au atoms connected to the boron framework separately. This indicates that the Au atoms prefer to bind atomically to negatively charged boron clusters.

3.2. PES spectra, Adiabatic ionization potentials and vertical detachment energies

As is well known, well-resolved PES spectra can serve as electronic “fingerprints” of the underlying clusters. To facilitate the experimental PES spectra, the simulated photoelectron spectroscopy spectra for anionic auroboranes are performed and displayed in Fig. S7 of supplementary information. As can be seen in Fig. S7, the simulated spectra of $\text{H}_2\text{B}_{11}^-$ and $\text{Au}_2\text{B}_{11}^-$ are compared with Li's²⁸ experimental spectra of $\text{H}_2\text{B}_{11}^-$. The numbers of distinct peaks of simulated photoelectron spectra in the low-binding-energy range of 2-4.6 eV and their relative positions overall agree with the experimental spectra. Those increase the confidence in the reliability of the ground-state structures isomers obtained. Unfortunately, only the experimental spectrum of $\text{H}_2\text{B}_{11}^-$ has been reported till now.

Furthermore, the adiabatic ionization potential (AIP) for Au_2B_9^+ , $\text{Au}_2\text{B}_{13}^+$ and vertical detachment energy (VDE) for the concerned anions $\text{Au}_2\text{B}_{10}^{2-}$, $\text{Au}_2\text{B}_{11}^-$, $\text{Au}_2\text{B}_{14}^{2-}$ and $\text{Au}_2\text{B}_{15}^-$ are calculated. The values are given at TPSS/Au/SDD/B/6-311+G* level, unless mentioned otherwise. The AIP is computed by following formula:

$$AIP = E_{\text{optimized cation}} - E_{\text{optimized neutral}} \quad (1)$$

Where $E_{\text{optimized cation}}$ and $E_{\text{optimized neutral}}$ are the total energies of corresponding clusters obtained at their respective ground-state geometries. Our results of adiabatic ionization potential (AIP) for cations Au_2B_9^+ and $\text{Au}_2\text{B}_{13}^+$ are summarized in Table 2. The optimized ground state structures of neutral Au_2B_9 and Au_2B_{13} are listed in Fig. S5 in supplementary information. It can be seen that Au_2B_9^+ and $\text{Au}_2\text{B}_{13}^+$ have significantly large ionization potentials (7.11 and 6.26 eV) at TPSS level, respectively. We recalculated the value of AIP for Au_2B_9^+ and $\text{Au}_2\text{B}_{13}^+$ at OVGf and CCSD(T)

levels, the obtained results are 5.66 (6.94) eV for Au_2B_9^+ and 5.72 (5.94) eV for $\text{Au}_2\text{B}_{13}^+$, respectively. The value in parentheses is obtained base on CCSD(T).

The vertical detachment energy (VDE) is defined as the energy difference between the anion and its unoptimized neutral counterpart both at the ground state geometry of the anionic cluster. The i th detachment energy (DE) is the energy required to remove the i th electron corresponding to i -valence anion change into $(i-1)$ -valence ion. Then, it might be given by the following definition:

$$DE^i = E_n^{i-1} - E_n^i \quad (2)$$

The DE^i is vertical if the E_n^{i-1} of corresponding cluster is the total energy of the unoptimized singly charged (neutral) cluster at the equilibrium geometry of the doubly (singly) charged anions. The VDE values for $\text{Au}_2\text{B}_{10}^{2-}$, $\text{Au}_2\text{B}_{11}^-$, $\text{Au}_2\text{B}_{14}^{2-}$ and $\text{Au}_2\text{B}_{15}^-$ clusters are listed in Table 2. From Table 2, we found that the energies required to remove one-electron from doubly charged $\text{Au}_2\text{B}_{10}^{2-}$ and $\text{Au}_2\text{B}_{14}^{2-}$ are 0.43 and 0.31 eV, respectively. These are much smaller than those (3.76 and 4.21 eV) of removing one electron from singly charged $\text{Au}_2\text{B}_{10}^-$ and $\text{Au}_2\text{B}_{14}^-$, suggesting that removing one electron from doubly charged anion is easier than from singly charged anion. In other words, the “second extra electron” is only weakly attached on these single charged anions. In addition, we also calculated the energies required to remove two-electrons from doubly charged $\text{Au}_2\text{B}_{10}^{2-}$ and $\text{Au}_2\text{B}_{14}^{2-}$. Their respective values are 3.23 and 4.46 eV, which implies that $\text{Au}_2\text{B}_{10}^{2-}$ and $\text{Au}_2\text{B}_{14}^{2-}$ dianions are more likely to lose one electron. For the singly charged $\text{Au}_2\text{B}_{11}^-$ and $\text{Au}_2\text{B}_{15}^-$, the calculated VDEs are 3.82 and 3.92 eV, respectively.

3.3. Fragmentation channels

The fragmentation energies of the lowest-energy isomers for Au_2B_9^+ , $\text{Au}_2\text{B}_{10}^{2-}$, $\text{Au}_2\text{B}_{11}^-$, $\text{Au}_2\text{B}_{13}^+$, $\text{Au}_2\text{B}_{14}^{2-}$ and $\text{Au}_2\text{B}_{15}^-$, were calculated at TPSS/Au/SDD/B/6-311+G* level. The results were compared with those of the corresponding H_2B_9^+ , $\text{H}_2\text{B}_{10}^{2-}$, $\text{H}_2\text{B}_{11}^-$, $\text{H}_2\text{B}_{13}^+$, $\text{H}_2\text{B}_{14}^{2-}$ and $\text{H}_2\text{B}_{15}^-$. The fragmentation energy is defined as the difference between a parent cluster and its daughters.⁵⁶

$$\Delta E_n^Q = \Delta E_{n-i}^Q + X_i - E_n^Q, \quad X = \text{Au or H}, \quad i=1 \text{ or } 2, \quad (3)$$

where n and Q denote the total number of clusters and different charge, respectively. Here, we mainly investigate two types of fragmentation channels; one is an Au (or H) atom dissociates and the other is that two gold atoms (or H₂ molecule) loss. All the fragmentation processes involving the corresponding detail fragmentation products and energies are listed in Table S1 of supplementary information.

For the sake of brevity, the ΔE of two channels for Au₂B₉⁺, Au₂B₁₀²⁻, Au₂B₁₁⁻, Au₂B₁₃⁺, Au₂B₁₄²⁻, Au₂B₁₅⁻ and the corresponding dihydride polyboroenes (H₂B₉⁺, H₂B₁₀²⁻, H₂B₁₁⁻, H₂B₁₃⁺, H₂B₁₄²⁻ and H₂B₁₅⁻) as a function of the cluster size are plotted in Fig. 3a and Fig. 3b, respectively. It can be seen that all the auropolyboroenes possess high fragmentation energies (about ≥ 3 eV) against the two type fragmentation channels. This appears to be comparable with the values of corresponding dihydride polyboroenes at the same theoretical level. The channels $Au_2B_n^Q = AuB_n^Q + Au$ for auropolyboroenes Au₂B₉⁺, Au₂B₁₀²⁻, Au₂B₁₃⁺ and Au₂B₁₄²⁻ have the lower fragmentation energies. However, for both singly charged anions Au₂B₁₁⁻ and Au₂B₁₅⁻, the fragmentation pathway $Au_2B_n^Q = B_n^Q + Au_2$ has the lower energies. Thus for $n = 11$ and 15 , the negative charge mainly resides on the B₁₁⁻ and B₁₅⁻ clusters during the dissociation. Additionally, the ΔE exhibits a maximum at $n = 14$, indicating that Au₂B₁₄²⁻ is less probable dissociation into B₁₄²⁻ and Au₂ due to one need to supply relatively high energy 5.40 eV. In the case of dihydride polyboroenes H₂B₉⁺, H₂B₁₀²⁻, H₂B₁₁⁻, H₂B₁₃⁺, H₂B₁₄²⁻ and H₂B₁₅⁻, we found that removing two H atoms of the ground state dihydride polyboroenes $H_2B_n^Q$ to produce an H₂ molecule plus a B_n^Q cluster is proved to have the lowest fragmentation energies. This may be due to the H₂ molecule is the most stable form for H atoms. Meanwhile, for all the dihydride boron clusters, the fragmentation energies of the fragmentation channel $H_2B_n^Q = HB_n^Q + H$ have very close values. Most strikingly, in the case of H₂B₁₄²⁻, the fragmentation energies of pathway $HB_{14}^{2-} + H$ is higher than that of $B_{14}^{2-} + H_2$ by only 0.04 eV (see Table S1).

3.4. Chemical bonding analyses

Next, we performed chemical bonding analyses for the lowest-energy isomers of considered auropolyborenes using the adaptive natural density partitioning (AdNDP) method.^{52, 53} AdNDP represents the molecular electronic structure in terms of n -center two-electron (nc -2e) bonds, including the familiar lone pairs (1c-2e) and localized 2c-2e bonds or delocalized nc -2e bonds ($3 \leq n \leq$ total numbers of atoms in the system). What's more, it is based on the concept that electron pairs are the main elements of the chemical bonds, which has been used successfully to analyze electronic structure and chemical bonding in previous literatures^{28, 57-59}. In order to keep the length of our paper, we only selected one isomer (Au_2B_9^+ , $\text{Au}_2\text{B}_{11}^-$ and $\text{Au}_2\text{B}_{14}^{2-}$) as example for each type with different charge (cation and singly/doubly charged anion). Results of the analysis are listed in Fig. 4, Fig. 5 and Fig. 6, respectively, where the blue and purple regions correspond to the different phases of the molecular wave functions for the MOs. Additionally, the calculated values of the bond order for nc -2e are marked by red text.

According to the AdNDP analysis, the ground state Au_2B_9^+ isomer (see Fig. 4) has ten lone pair (1c-2e) Au atomic 5d-orbitals with occupy number (ON) in the range of 1.81-1.99 |e|. The remaining 26 electrons form seven 2c-2e localized B-B σ -bonds (ON = 1.80-1.92 |e|), one 3c-2e Au-Au-B σ -bonds (ON = 1.98 |e|), three 4c-2e B-B-B-B σ -bonds and two 4c-2e B-B-B-B delocalized over four boron atoms' π -bonds (ON = 1.84-1.88 |e|). We found Au_2B_9^+ isomer possesses two 4c-2e π (four π electrons) bonds. However, it can be seen that these 3c-2e and 4c-2e bonds are very weak as revealed by the calculated bond orders, and hence the bonds in this cluster are mainly described as 2c-2e localized B-B σ -bonds and Au d-orbitals. This may be used to explain the reason why the structure of this cluster is nonplanar and different from the ground state of H_2B_9^+ . Additionally, this structure may provide some occupation of s- and p-AOs of boron, avoiding the presence of any unoccupied atomic orbital.

For the anionic $\text{Au}_2\text{B}_{11}^-$ (see Fig. 5), AdNDP analysis reveals clearly the existence of ten 1c-2e Au 5d lone-pairs (d_{xy} , d_{xz} , d_{yz} , $d_x^2 - y^2$ and d_z^2 on each Au atom), which is similar to the 1c-2e bonding picture of Au_2B_9^+ . In addition, there are two

2c-2e Au-B σ -bonds, six 2c-2e B-B localized σ -bonds, two 4c-2e B-B-B-B π -bonds with the adjacent B₂ pair in each B₄ and one 5c-2e B-B-B-B-B π -bond. Three π -bonds (six π -electrons) in the boron framework is π aromatic according to the Hückel $4n+2$ rule⁶⁰. This is similar to the H₂B₁₁⁻ presented by Li et al.²⁸, and three π orbitals should be also compared with those of 1, 3, 5-hexatriene. However, the elongated shape of Au₂B₁₁⁻ is not consistent with π aromaticity. More interestingly, we found that there are five 3c-2e B-B-B and two 5c-2e B-B-B-B-B σ -bonds in this cluster. The latter bonding features give rise to double aromaticity for Au₂B₁₁⁻ cluster because each number of π or σ electrons satisfies the Hückel $4n+2$ rule. Thus, this cluster possesses structure stabilized by electron delocalization both in the π or σ framework. By calculating the bond order, we found that three 3c-2e B-B-B σ -bonds in the center of boron framework are much stronger comparing with the others in two sides. Among the three 5c-2e B-B-B-B-B bonds, only one 5c-2e σ -bond has large bond order 0.11, whereas others are nearly zero. Moreover, the bonding patterns of 2c-2e, 3c-2e, 4c-2e and 5c-2e for Au₂B₁₁⁻ cluster are very similar to those of H₂B₁₁⁻ (see Fig. S6 in supplementary information). This further supports the Au/H analogy in Au alloy clusters.

As for the Au₂B₁₄²⁻, ten 1c-2e Au 5d-orbitals are similar to those observed in both Au₂B₉⁺ and Au₂B₁₁⁻ clusters. The two rows of boron atoms in the ladder structure are bonded via multicenter σ and π bonds. The bond pattern between the two Au atoms and the boron framework is σ bond. Additionally, eight 2c-2e B-B σ -bonds (ON = 1.82-1.99 |e|), six 3c-2e B-B-B σ -bonds (ON = 1.97 |e|), and two 4c-2e B-B-B-B σ -bonds (ON = 1.90 |e|) are observed in this cluster. It is worth pointing out that the four middle 3c-2e B-B-B σ -bonds are much stronger than the two others with bond order -1.68. Meanwhile, the two 4c-2e B-B-B-B σ -bonds with bond order 0.14 are also significantly strong compared with the two 4c-2e π -bonds. Two 5c-2e B-B-B-B-B π -bonds and two 5c-2e B-B-B-B-B σ -bonds are all very weak according to the calculated bond order. Just like Au₂B₁₁⁻, we found the Au₂B₁₄²⁻ cluster with three delocalized π bonds (six π electrons) is also π aromatic, while Au₂B₁₄²⁻ is an σ antiaromatic due to it has eighteen σ bonds fulfilling the Hückel $4n$ rule for

antiaromaticity. This may be the reason why $\text{Au}_2\text{B}_{14}^{2-}$ gains major stabilization to the ground state. By the comparison between chemical bonding of $\text{Au}_2\text{B}_{14}^{2-}$ and $\text{H}_2\text{B}_{14}^{2-}$ (Fig. S6), we found that their major bonds are the same especially for the bonds of Au-B and H-B.

In conclusion, the π bonds in auropolyborenes Au_2B_9^+ , $\text{Au}_2\text{B}_{11}^-$ and $\text{Au}_2\text{B}_{14}^{2-}$ are delocalized only over parts of the boron frameworks. There is no longer a complete ring of 2c-2e B-B σ bonds found in all boron clusters, whereas there are some 3c-2e B-B-B σ bonds exist. $\text{Au}_2\text{B}_{11}^-$ and $\text{Au}_2\text{B}_{14}^{2-}$ anions can be considered as covalent complexes between π aromatic B_{11}^- and B_{14}^{2-} core and two monovalent σ -radicals Au, which are connected by two B-Au σ -bonds. Additionally, the bonding patterns of auropolyborenes bear similarities to those in dihydride polyborenes which have the similar structures with auropolyborenes, especially for the Au-B and H-B bondings. This further supports the Au/H analogy in our studied complexes.

4. Conclusions

In summary, we have presented a systematic study on the equilibrium geometries, electronic structure, thermodynamic stability, and chemical bonding analysis of the auropolyborenes $[\text{Au}_2(\text{B}_4)_x\text{B}_3]^-$, $[\text{Au}_2(\text{B}_4)_x\text{B}_2]^{2-}$ and $[\text{Au}_2(\text{B}_4)_x\text{B}]^+$ ($x = 2, 3$), comparing with the corresponding dihydride polyborenes. All the results are summarized as follows:

- (1) Based on the geometry optimization, the ladderlike structures are proved to be the ground states for $\text{Au}_2\text{B}_{10}^{2-}$, $\text{Au}_2\text{B}_{11}^-$, $\text{Au}_2\text{B}_{14}^{2-}$ and $\text{Au}_2\text{B}_{15}^-$ at TPSS, OVGf and CCSD(T) levels, which are similar to the corresponding dihydride polyborenes $\text{H}_2\text{B}_{10}^{2-}$, $\text{H}_2\text{B}_{11}^-$, $\text{H}_2\text{B}_{14}^{2-}$ and $\text{H}_2\text{B}_{15}^-$. These auropolyborenes and dihydride polyborenes could be potential nanowires.
- (2) To facilitate the experimental PES spectra, the simulated photoelectron spectroscopy spectra for anionic clusters were performed. We also calculated the AIPs for cations and VDEs for the concerned anions. The calculated VDEs for the $\text{Au}_2\text{B}_{10}^{2-}$ and $\text{Au}_2\text{B}_{14}^{2-}$ dianions show that removing one electron from dianions is easier than from singly charged $\text{Au}_2\text{B}_{10}^-$ and $\text{Au}_2\text{B}_{14}^-$. That is to say, these two dianions are more likely to lose one electron. Meanwhile, the fragmentation

channels and products are deeply discussed.

- (3) Using the AdNDP method, we take Au_2B_9^+ , $\text{Au}_2\text{B}_{11}^-$ and $\text{Au}_2\text{B}_{14}^{2-}$ as examples to analyze their electronic structure and chemical bonding. The results reveal that the π -bonds are delocalized only over parts of the boron frameworks. $\text{Au}_2\text{B}_{11}^-$ and $\text{Au}_2\text{B}_{14}^{2-}$ can be regarded as covalent complexes between a π aromatic core (B_{11}^- or B_{14}^{2-}) and two monovalent σ -radicals Au. Noteworthy is the fact that the chemical bonding patterns of auroboroenes bear similarities to these in dihydride polyboroenes especially for Au-B and H-B bonding.

Acknowledgements

This work was supported by the Shaanxi University of Science & Technology Key Research Grant (No.BJ15-07).

References

- 1 N. N. Greenwood and A. Earnshaw, *Chemistry of the Elements*, 2nd ed. Butterworth-Heinemann.: Oxford, 1997.
- 2 F. A. Cotton, G. Wilkinson, C. A. Murrillo and M. Bochmann, *Advanced Inorganic Chemistry* (6th ed) John Wiley & Sons.: New York, 1999.
- 3 I. Boustani, *Int. J. Quant. Chem.*, 1994, **52**, 1081-1111; I. Boustani, *Phys. Rev. B*, 1997, **55**, 16426-16438.
- 4 J. I. Aihara, H. Kanno and T. Ishida, *J. Am. Chem. Soc.*, 2005, **127**, 13324-13330; J. O. C. Jimenez-Halla, R. Islas, T. Heine and G. Merino, *Angew. Chem., Int. Ed.*, 2010, **49**, 5668-5671.
- 5 J. E. Fowler and J. M. Ugalde, *J. Phys. Chem. A*, 2000, **104**, 397-403.
- 6 J. Aihara, *J. Phys. Chem. A*, 2001, **105**, 5486-5489.
- 7 B. Kiran, G. G. Kumar, M. T. Nguyen, A. K. Kandalam and P. Jena, *Inorg. Chem.*, 2009, **48**, 9965-9967.
- 8 H. J. Zhai, B. Kiran, J. Li and L. S. Wang, *Nature Mater.*, 2003, **2**, 827-833.

- 9 H. J. Zhai, A. N. Alexandrova, K. A. Birch, A. I. Boldyrev and L. S. Wang, *Angew. Chem., Int. Ed.*, 2003, **42**, 6004-6008; A. N. Alexandrova, H. J. Zhai, L. S. Wang and A. I. Boldyrev, *Inorg. Chem.*, 2004, **43**, 3552-3554.
- 10 A. P. Sergeeva, B. B. Averkiev, H. J. Zhai, A. I. Boldyrev and L. S. Wang, *J. Chem. Phys.*, 2011, **134**, 224304-224315.
- 11 A. P. Sergeeva, D. Yu. Zubarev, H. J. Zhai, A. I. Boldyrev and L. S. Wang, *J. Am. Chem. Soc.*, 2008, **130**, 7244-7246; W. Huang, A. P. Sergeeva, H. J. Zhai, B. B. Averkiev, L. S. Wang and A. I. Boldyrev, *Nature Chem.*, 2010, **2**, 202-206; Z. A. Piazza, W. L. Li, C. Romanescu, A. P. Sergeeva, L. S. Wang and A. I. Boldyrev, *J. Chem. Phys.*, 2012, **136**, 104310-104318; A. P. Sergeeva, Z. A. Piazza, C. Romanescu, W. L. Li, A. I. Boldyrev and L. S. Wang, *J. Am. Chem. Soc.*, 2012, **134**, 18065-18073.
- 12 B. Kiran, S. Bulusu, H. J. Zhai, S. Yoo, X. C. Zeng and L. S. Wang, *Proc. Natl. Acad. Sci. USA*, 2005, **102**, 961-964.
- 13 A. N. Alexandrova, A. I. Boldyrev, H. J. Zhai and L. S. Wang, *Coord. Chem. Rev.*, 2006, **250**, 2811-2866.
- 14 D. Yu. Zubarev and A. I. Boldyrev, *J. Comput. Chem.*, 2007, **28**, 251-268.
- 15 E. Oger, N. R. M. Crawford, R. Kelting, P. Weis, M. M. Kappes and R. Ahlrichs, *Angew. Chem., Int. Ed.*, 2007, **46**, 8503-8506.
- 16 L. Hanley, J. L. Whitten and S. L. Anderson, *J. Phys. Chem.*, 1988, **92**, 5803-5814; P. A. Hintz, S. A. Ruatta and S. L. Anderson, *J. Chem. Phys.*, 1990, **92**, 292-303; S. A. Ruatta, P. A. Hintz and S. L. Anderson, *J. Chem. Phys.*, 1991, **94**, 2833-2847; M. B. Sowa-Resat, J. Smolanoff, A. Lapiki and S. L. Anderson, *J. Chem. Phys.*, 1997, **106**, 9511-9522.
- 17 W. N. Lipscomb, *Boron Hydrides*, Benjamin.: New York, 1963; W. N. Lipscomb, *Sci.*, 1977, **196**, 1047-1055.
- 18 R. P. Bell and H. C. Longuet-Higgins, *Nature.*, 1945, **155**, 328-329.
- 19 W. H. Eberhardt, B. Crawford and W. N. Lipscomb, *J. Chem. Phys.* 1954, **22**, 989-1001.
- 20 (a) K. P. Hall and D. M. P. Mingos, *Prog. Inorg. Chem.*, 1984, **32**, 237-254; (b) J.

- K. Burdett, O. Eisenstein and W. B. Schweizer, *Inorg. Chem.*, 1994, **33**, 3261-3268.
- 21 K. P. Hall and D. M. P. Mingos, *Prog. Inorg. Chem.*, 1984, **32**, 237-254.
- 22 H. J. Zhai, L. S. Wang, D. Yu. Zubarev and A. I. Boldyrev, *J. Phys. Chem. A*, 2006, **110**, 1689-1693.
- 23 D. Y. Zu, J. Li, L.-S. W and A. I. Boldyev, *Inorg. Chem.*, 2006, **45**, 5269-5271.
- 24 H. J. Zhai, C. Q. Miao, S. D. Li, and L. S. Wang, *J. Phys. Chem. A*, 2010, **114**, 12155-12161.
- 25 D. Z. Li and S. D. Li, *Int. J. Quantum Chem.*, 2011, **111**, 4418-4424.
- 26 W. Z. Yao, D. Z. Li, and S. D. Li, *J. Comput. Chem.*, 2011, **32**, 218-225.
- 27 Q. Chen, H. J. Zhai, S. D. Li and L. S. Wang, *J. Chem. Phys.*, 2013, **138**, 084306-084313.
- 28 W. L. Li, C. Romanescu, T. Jian and L. S. Wang, *J. Am. Chem. Soc.* 2012, **134**, 13228-13231.
- 29 J. Tao, J. P. Perdew, V. N. Staroverov and G. E. Scuseria, *Phys. Rev. Lett.*, 2003, **91**, 146401-146405.
- 30 M. J. Frisch, G. W. Trucks and H. B. Schlegel, et al., *Gaussian 09* (Revision C.0), Gaussian, Inc., Wallingford, CT, 2009.
- 31 P. Schwerdtfeger, M. Dolg, W. H. E. Schwarz, G. A. Bowmaker and P. D. W. Boyd, *J. Chem. Phys.*, 1989, **91**, 1762-1774.
- 32 R. Krishnan, J. S. Binkley, R. Seeger and J. A. Pople, *J. Chem. Phys.*, 1980, **72**, 650-654.
- 33 A. D. Becke, *J. Chem. Phys.*, 1993, **98**, 5648-5652.
- 34 J. P. Perdew and Y. Wang, *Phys. Rev. B: Condens. Matter.*, 1992, **45**, 13244-13249.
- 35 J. P. Perdew, P. Ziesche and H. Eschrig, *Electronic Structure of Solids*, ed. Akademie Verlag.: Berlin, 1991.
- 36 J. P. Perdew, K. Burke and M. Ernzerhof, *Phys. Rev. Lett.*, 1996, **77**, 3865-3868.
- 37 A. D. Becke, *Phys. Rev. A*, 1988, **38**, 3098-3100.
- 38 Y. Zhao and D. G. Truhlar, *J. Phys. Chem. A*, 2006, **110**, 13126-13130.
- 39 G. D. Purvis and R. J. Bartlett, *J. Chem. Phys.*, 1982, **76**, 1910-1918.

- 40 G. E. Scuseria, C. L. Janssen and H. F. Schaefer III, *J. Chem. Phys.*, 1988, **89**, 7382-7387.
- 41 G. E. Scuseria and H. F. Schaefer III, *J. Chem. Phys.*, 1989, **90**, 3700-3703.
- 42 K. P. Huber and G. Herzberg, *Constants of Diatomic Molecules*, New York.: Van Nostrand Reinhold, 1979.
- 43 D. R. Lide, *CRC Handbook of chemistry and physics 87th edn*, New York.: CRC Press, 2006.
- 44 B. Rosen, *Spectroscopic Data Relative to Diatomic Molecules*, Oxford.: Pergamon, 1970.
- 45 N. Akman, M. Tas, C. Oözdoğan and I. Boustani, *Phys. Rev. B*, 2011, **84**, 075463-075473.
- 46 T. B. Tai, N. M. Tam and M. T. Nguyen, *Theor. Chem. ACC.*, 2012, **131**, 1241-1256.
- 47 H. J. Zhai, B. Kiran, J. Li and L.-S. Wang, *Nature*, 2003, **2**, 827-833.
- 48 R. J. Bartlett and M. Musial, *Rev. Mod. Phys.*, 2007, **79**, 291-352.
- 49 L. S. Cederbaum, *J. Phys. B*, 1975, **8**, 290-303.
- 50 J. V. Ortiz, *J. Chem. Phys.*, 1996, **104**, 7599-7605.
- 51 V. G. Zakrzewski and W. von Niessen, *J. Comp. Chem.*, 1993, **14**, 13-18.
- 52 D. Y. Zubarev and A. I. Boldyrev, *Phys. Chem. Chem. Phys.*, 2008, **10**, 5207-5217.
- 53 D. Y. Zubarev and A. I. Boldyrev, *J. Org. Chem.*, 2008, **73**, 9251-9258.
- 54 T. Lu and F. W. Chen, *J. Comput. Chem.*, 2012, **33**, 580-592.
- 55 R. Dennington, T. Keith, J. Millam, GaussView, version 5.0.8; Semichem, Inc.: Shawnee Mission, KS, 2007.
- 56 B. K. Rao, P. Jena, M. Manninen and R. M. Nieminen, *Phys. Rev. Lett.*, 1987, **58**, 1188-1191.
- 57 C. Romanescu, T. R. Galeev, W. L. Li, A. Boldyrev and L. S. Wang, *Accounts. Chem. Res.*, 2013, **46**, 350-358.
- 58 J. K. Olson and A. I. Boldyrev, *J. Phys. Chem. A*, 2013, **117**, 1614-1620.
- 59 H. Bai, H. J. Zhai, S. D. Li and L. S. Wang, *Phys. Chem. Chem. Phys.*, 2013, **15**,

9646-9653

60 M. J. Goldstein, *J. Am. Chem. Soc.*, 1967, **89**, 6357-6359.**Table 1.** The bond length (r) and vibrational frequency (ω) of the binary clusters B_2 , Au_2 , AuB and AuB^- at different levels.

Au_2 ($^1\Sigma_g^-$ $D_{\infty h}$)									
	B3LYP	B3PW91	TPSS	PBE	BPW91	PW91	M06	CCSD	Exp./Theo.
r	2.58	2.55	2.55	2.56	2.56	2.56	2.60	2.57	2.47^a
ω	163	169	171	166	166	167	160	172	191^a
B_2 ($^5\Sigma_u^-$ $D_{\infty h}$)									
r	1.52	1.52	1.53	1.53	1.53	1.53	1.52	1.53	1.59^b
ω	1280	1285	1240	1244	1246	1245	1298	1263	1052^c
AuB ($^1\Sigma^+$ $C_{\infty v}$)									
r	1.95	1.95	1.95	1.94	1.94	1.94	1.98	1.93	1.95^d
ω	634	646	655	660	653	660	589	661	—
AuB^- ($^2\Sigma^+$ $C_{\infty v}$)									
r	2.01	2.00	2.00	1.99	1.99	1.99	2.04	1.97	1.99^d
ω	525	543	544	568	558	567	497	574	—

^{a, b, c}Experiment Ref 42, 43, 44.^dTheoretical studied bond length Ref 25.

Table 2. Adiabatic ionization potentials (AIP) for the ground state of Au_2B_9^+ , $\text{Au}_2\text{B}_{13}^+$ and vertical detachment energy (VDE) for the anions $\text{Au}_2\text{B}_{10}^{2-}$, $\text{Au}_2\text{B}_{11}^-$, $\text{Au}_2\text{B}_{14}^{2-}$, $\text{Au}_2\text{B}_{15}^-$ at TPSS/Au/SDD/B/6-311+G* level.

	species					
	Au_2B_9^+	$\text{Au}_2\text{B}_{13}^+$	$\text{Au}_2\text{B}_{10}^{2-}$	$\text{Au}_2\text{B}_{14}^{2-}$	$\text{Au}_2\text{B}_{11}^-$	$\text{Au}_2\text{B}_{15}^-$
AIP	7.11	6.26	—	—	—	—
VDE	—	—	0.43 ^a , 3.76 ^b	0.31 ^a , 4.21 ^b	3.82	3.92

^aThe energy required to remove one electron from doubly charged $\text{Au}_2\text{B}_{10}^{2-}$ and $\text{Au}_2\text{B}_{14}^{2-}$ clusters. ^bThe energy required to remove one electron from singly charged $\text{Au}_2\text{B}_{10}^-$ and $\text{Au}_2\text{B}_{14}^-$.

Fig. 1 Optimized structures of multicharged B_9^+ , B_{10}^{2-} , B_{11}^- , B_{13}^+ , B_{14}^{2-} and B_{15}^- clusters.

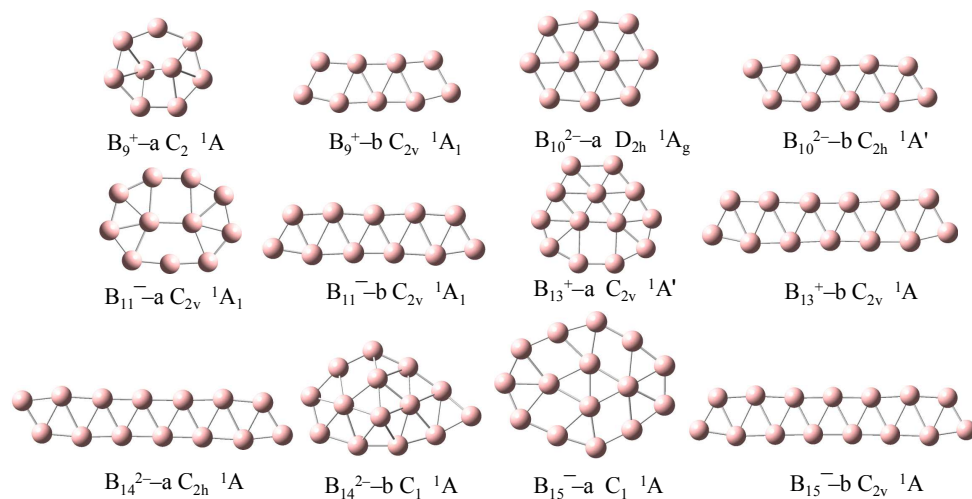


Fig. 2 Optimized structures of auropolyborenes $[\text{Au}_2(\text{B}_4)_x\text{B}_3]^-$, $[\text{Au}_2(\text{B}_4)_x\text{B}_2]^{2-}$ and $[\text{Au}_2(\text{B}_4)_x\text{B}]^+$ ($x = 2, 3$) with their symmetry, electron state, and relative energies at the OVGF/Au/SDD/B/6-311+G* method in curly brackets, those at the CCSD(T)/Au/SDD/B/6-311+G* level in parentheses, and those otherwise at B3LYP/Au/SDD/B/6-311+G*.

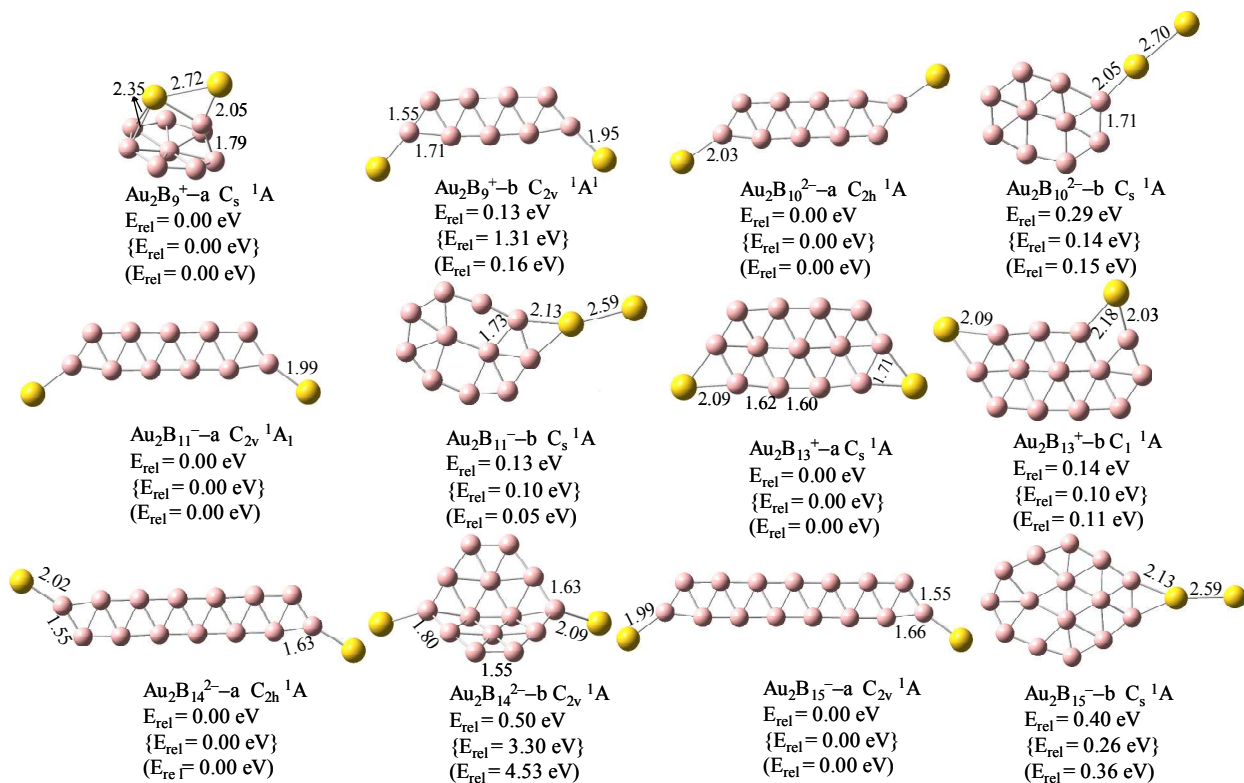


Fig. 3 (a) Dissociation energies for two fragmentation channels of various auropolyborenes $Au_2B_n^Q$. (b) Dissociation energies for two fragmentation channels of dihydride polyborenes $H_2B_n^Q$.

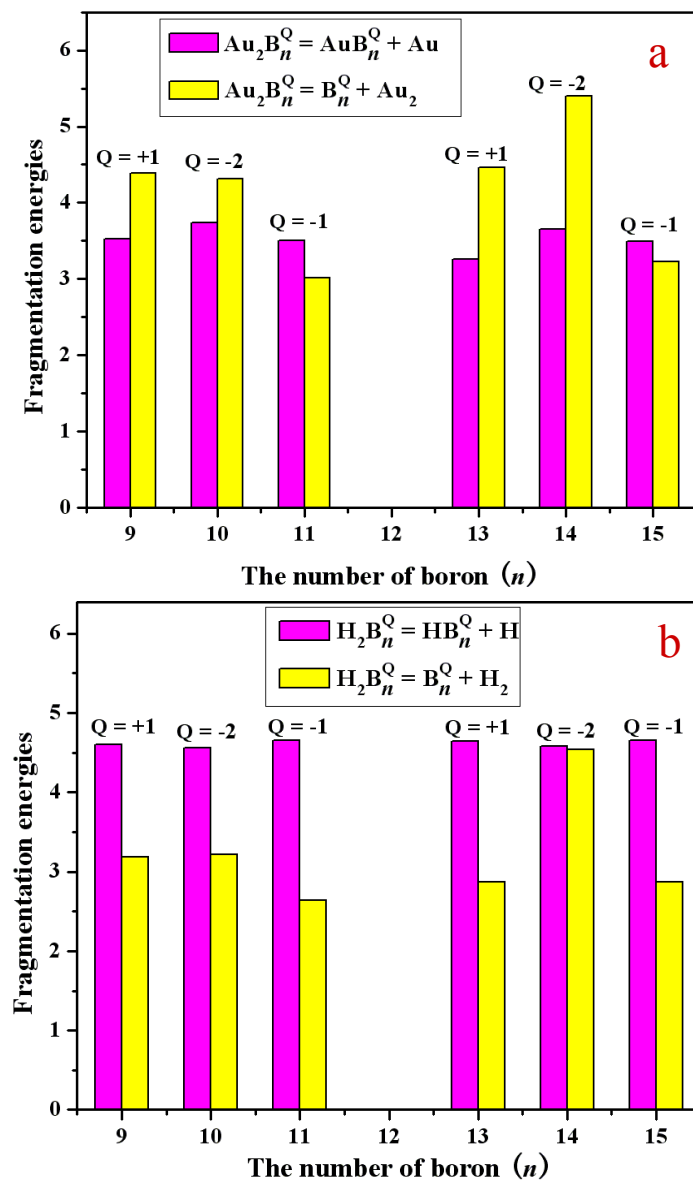


Fig. 4 Chemical bonding analyses for Au_2B_9^+ auropolyboroene using the AdNDP method.

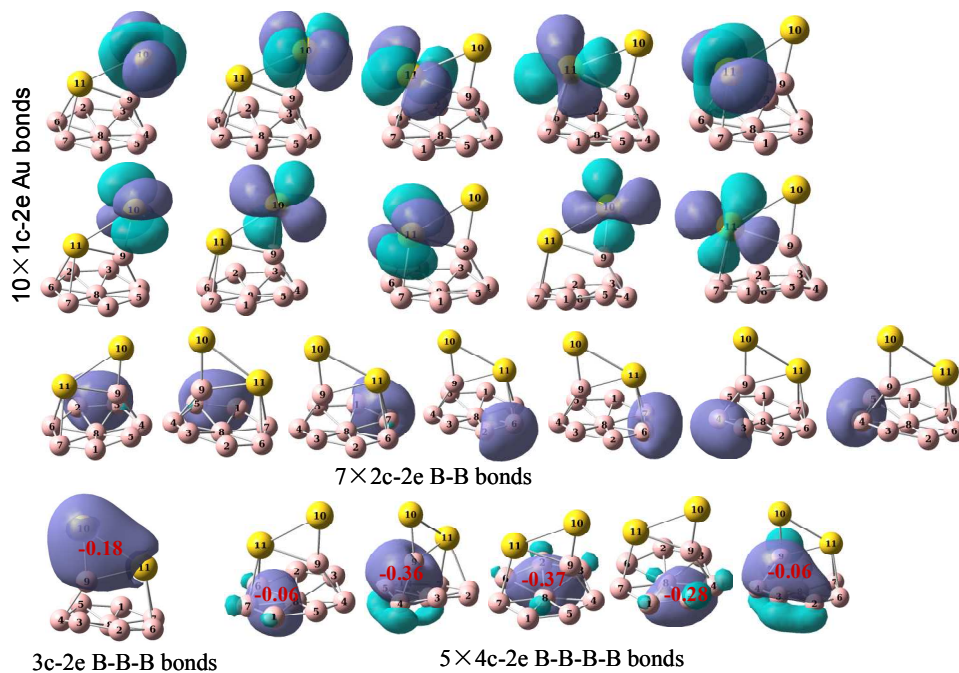


Fig. 5 Chemical bonding analyses for $\text{Au}_2\text{B}_{11}^-$ auropolyboroene using the AdNDP method.

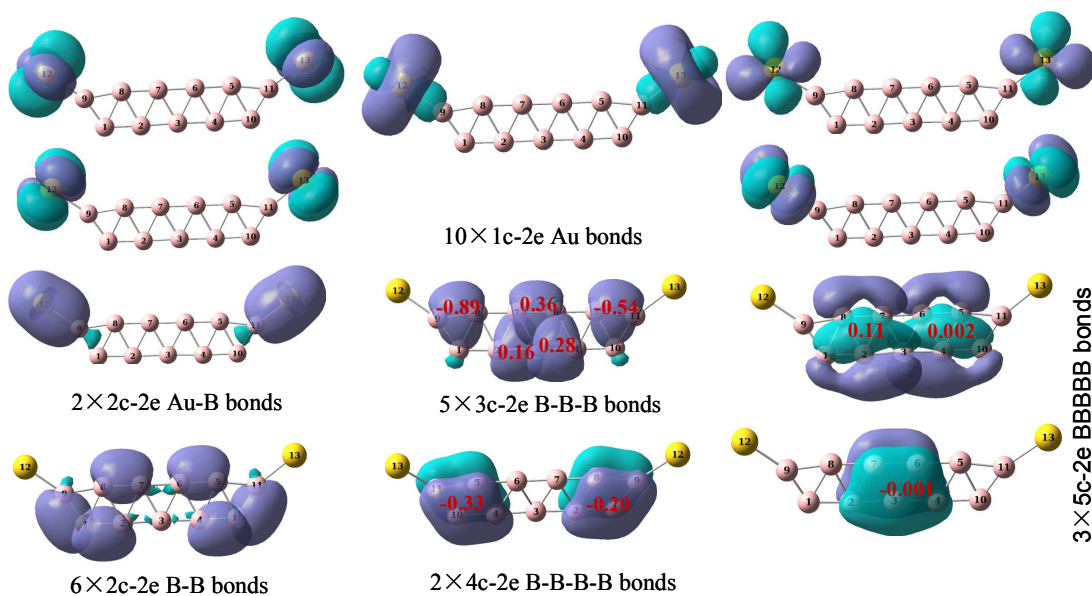


Fig. 6 Chemical bonding analyses for $\text{Au}_2\text{B}_{14}^{2-}$ auropolyborene using the AdNDP method.

